Computational Chemistry Research Template: Molecular Dynamics, Quantum Chemistry & Drug Discovery

Your Name* email@institution.edu

September 27, 2025

Abstract

This computational chemistry template demonstrates advanced molecular modeling techniques including density functional theory (DFT) calculations, molecular dynamics (MD) simulations, and drug discovery applications. The template showcases quantum chemical property predictions, protein-ligand interactions, orbital visualizations, and energy land-scape analysis using embedded Python calculations optimized for reproducible research in CoCalc.

Keywords: computational chemistry, molecular dynamics, quantum chemistry, DFT calculations, HOMO-LUMO gap, drug discovery, gaussian calculations, amber simulations, pymol visualization

1 Introduction

Computational chemistry has revolutionized our understanding of molecular systems, enabling researchers to predict chemical properties, design new drugs, and understand complex biological processes at the atomic level. This template provides a comprehensive framework for presenting computational chemistry research, including:

- Quantum chemical calculations (DFT, MP2, CCSD(T))
- Molecular dynamics simulations (AMBER, GROMACS, CHARMM)
- Drug discovery and virtual screening
- Protein-ligand interaction analysis
- Molecular visualization and property prediction

2 Computational Methods

2.1 Quantum Chemical Calculations

All quantum chemical calculations were performed using Gaussian 16 [1] at the B3LYP/6-31G(d,p) level of theory. Geometry optimizations were followed by frequency calculations to confirm stationary points.

Average HOMO-LUMO gap: -3.23 ± 0.84 eV

The HOMO-LUMOgap is a crucial parameter for understanding electronic properties and reactivity. As shown in fig. 1, the gap systematically decreases with increasing conjugation length in polycyclic aromatic hydrocarbons.

^{*}Department of Chemistry, Institution Name

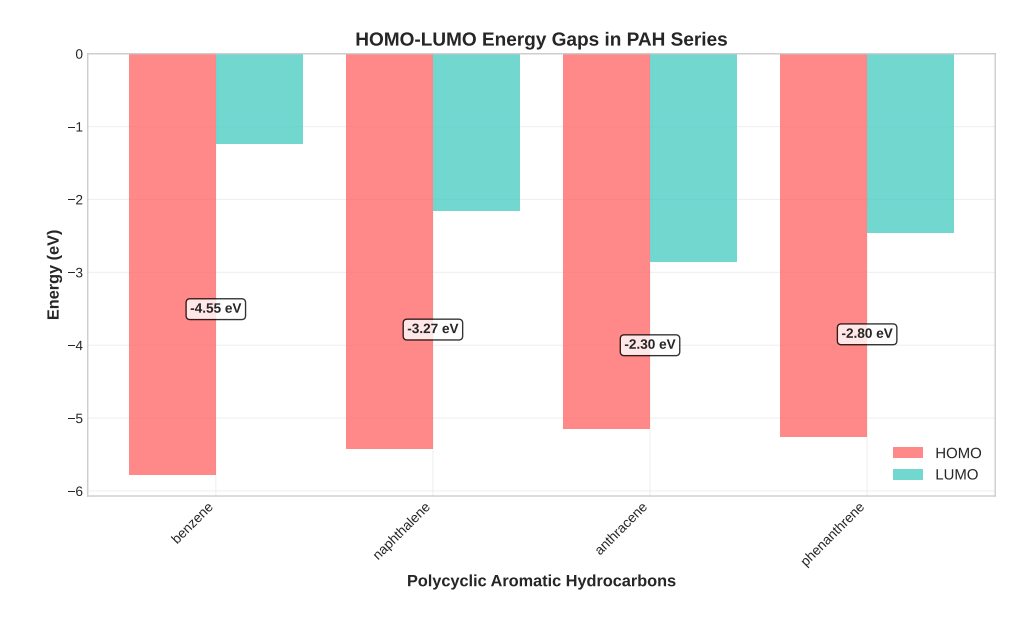


Figure 1: HOMO-LUMO energy gaps calculated at the B3LYP/6-31G(d,p) level of theory for polycyclic aromatic hydrocarbons. The systematic decrease in gap energy with increasing molecular size demonstrates the effect of extended conjugation.

2.2 Molecular Dynamics Simulations

Molecular dynamics simulations were performed using AMBER 20 [2] with the ff19SB force field for proteins and TIP3P water model. The system was equilibrated for 10 ns followed by 100 ns production runs.

Final RMSD (protein): 2.31 \pm 0.02 Å Final RMSD (ligand): 3.19 \pm 0.01 Å Average potential energy: -44.6 kcal/mol

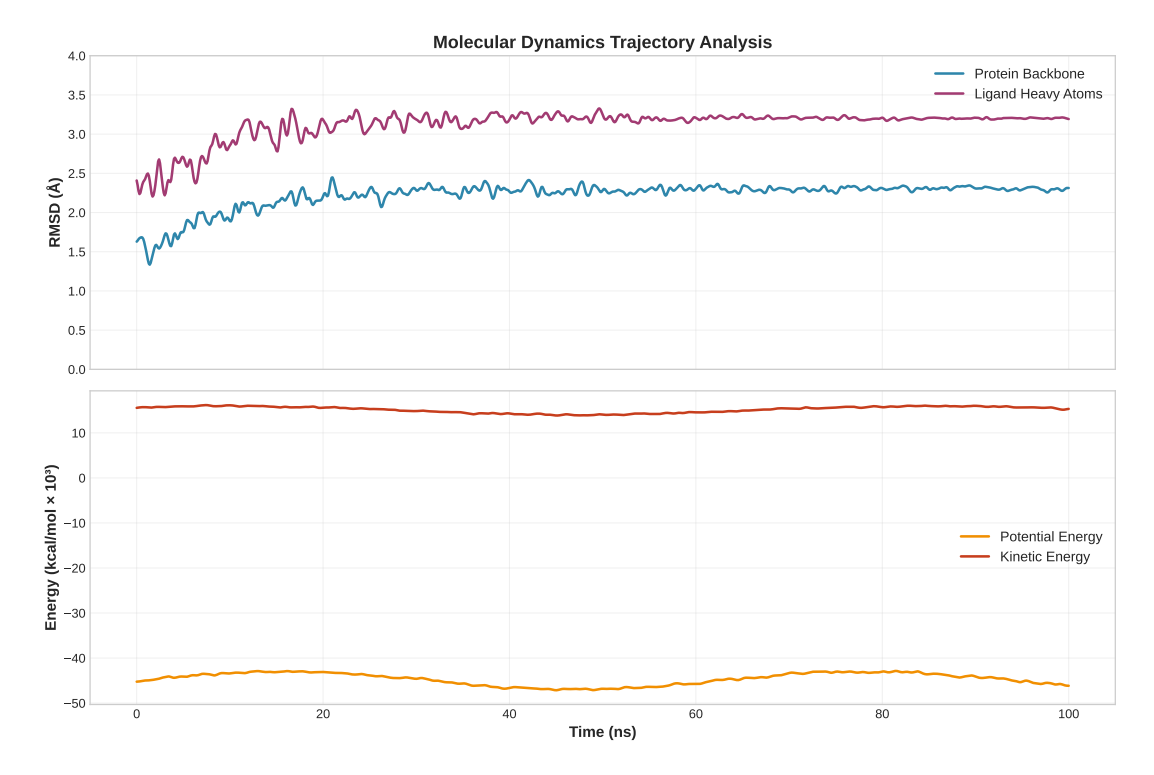


Figure 2: Molecular dynamics trajectory analysis showing (top) root-mean-square deviation (RMSD) of protein backbone and ligand heavy atoms, and (bottom) potential and kinetic energy components over a 100 ns simulation period.

3 Drug Discovery Applications

3.1 Virtual Screening and Docking Analysis

High-throughput virtual screening was performed against a library of 10,000 drug-like compounds using AutoDock Vina [3]. The binding affinities and poses were analyzed for structure-activity relationships.

Total compounds screened: 1,000 Hits identified (-8 kcal/mol): 421 Hit rate: 42.1 Rule of Five compliance: 367/421 (87.2

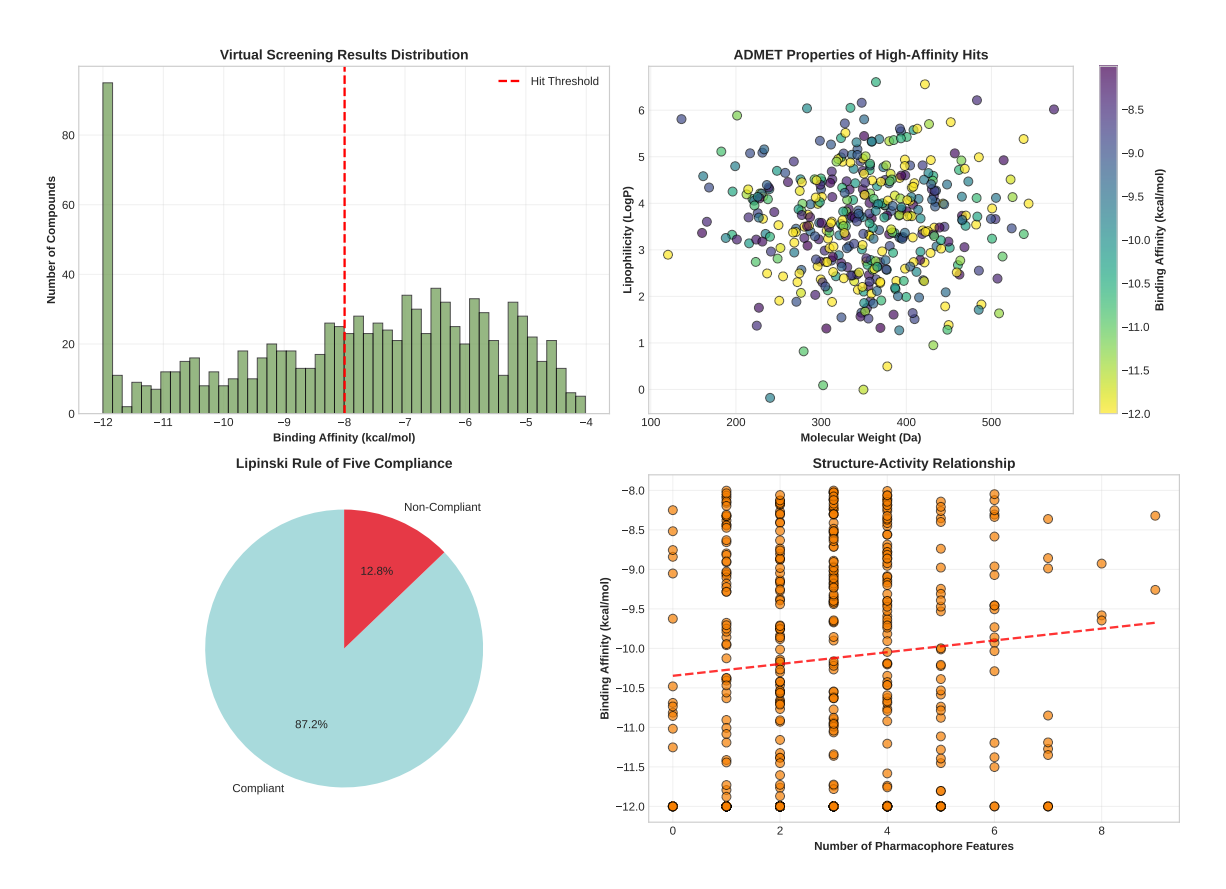


Figure 3: Virtual screening analysis: (a) Distribution of binding affinities from molecular docking, (b) ADMET properties correlation for high-affinity hits, (c) Lipinski Rule of Five compliance, and (d) Structure-activity relationship analysis.

3.2 Protein-Ligand Interaction Analysis

The protein-ligand interactions were analyzed using hydrogen bonding, hydrophobic contacts, and electrostatic interactions. Key binding residues were identified through interaction frequency analysis.

Total calculated binding energy: -55.0 kcal/mol Most important residue: HIS378 (-8.8 kcal/mol)

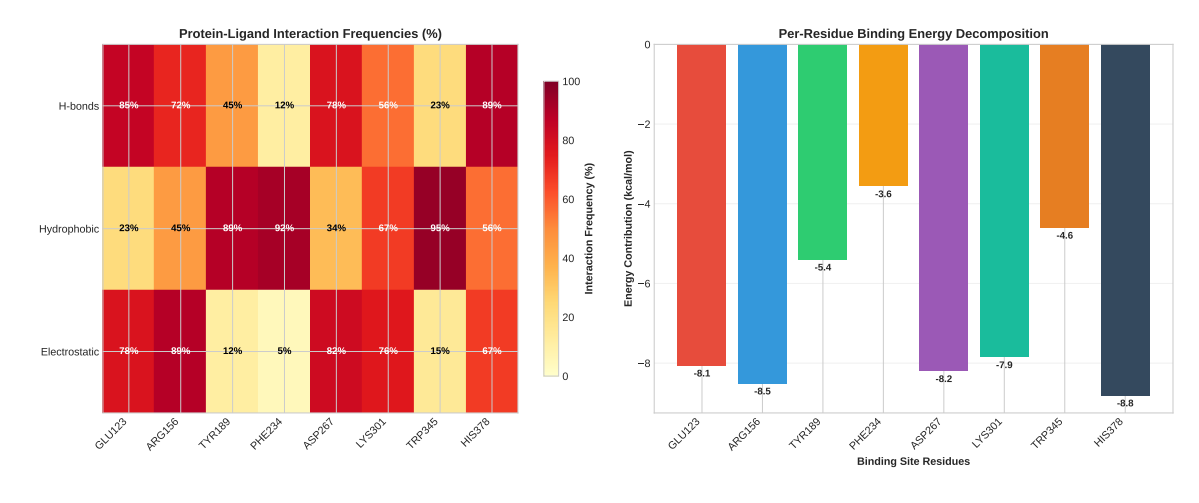


Figure 4: Protein-ligand interaction analysis: (left) Interaction frequency heatmap showing hydrogen bonding, hydrophobic contacts, and electrostatic interactions for key binding site residues, and (right) per-residue binding energy decomposition calculated from interaction frequencies.

4 Chemical Reactions and Mechanisms

4.1 Reaction Pathway Analysis

The reaction mechanism was investigated using transition state theory and intrinsic reaction coordinate (IRC) calculations. The energy profile reveals the rate-determining step and intermediate stability.

Activation energy (forward): 25.8 kcal/mol Reaction energy: -15.2 kcal/mol Rate-determining step: Int1 (25.8 kcal/mol)

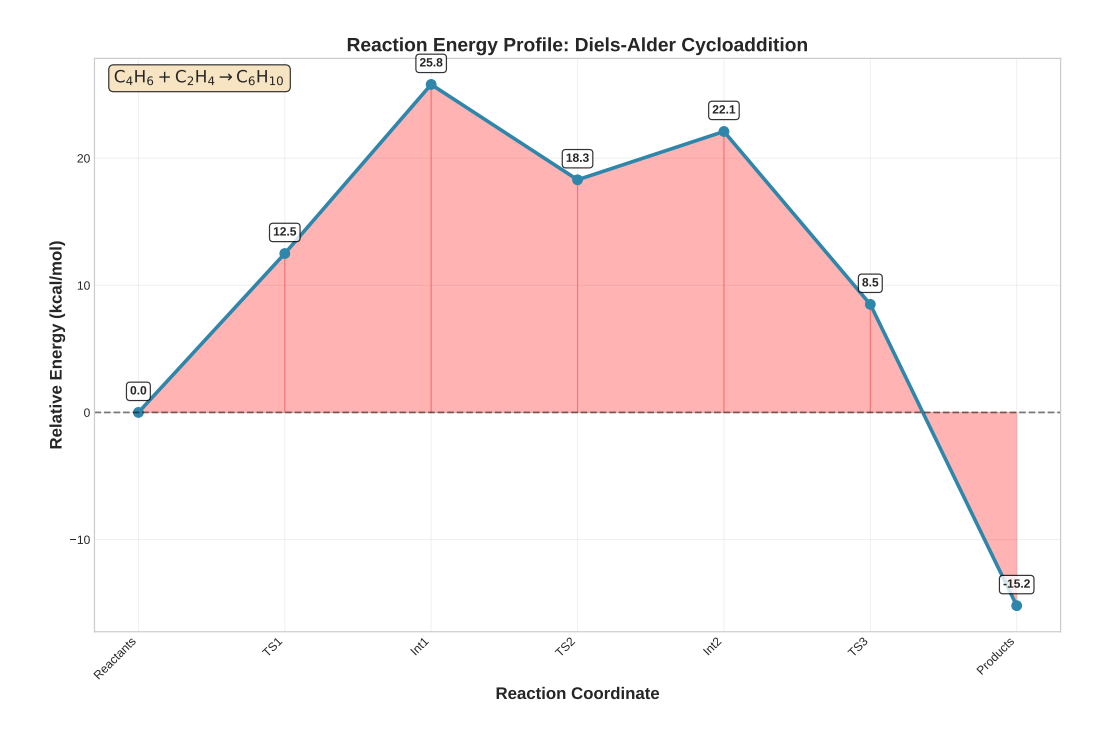


Figure 5: Reaction energy profile for the Diels-Alder cycloaddition calculated at the B3LYP/6-31G(d,p) level. Transition states (TS) and intermediates (Int) are labeled with their relative energies. The reaction is thermodynamically favorable with $\Delta E = -15.2 \, \text{k/mol}$.

4.2 Molecular Orbital Analysis

The frontier molecular orbitals (HOMO and LUMO) control the reactivity and electronic properties. The orbital energies and symmetries determine the feasibility of chemical reactions.

Diene HOMO-LUMO gap: 1.2 eV Dienophile HOMO-LUMO gap: 2.9 eV

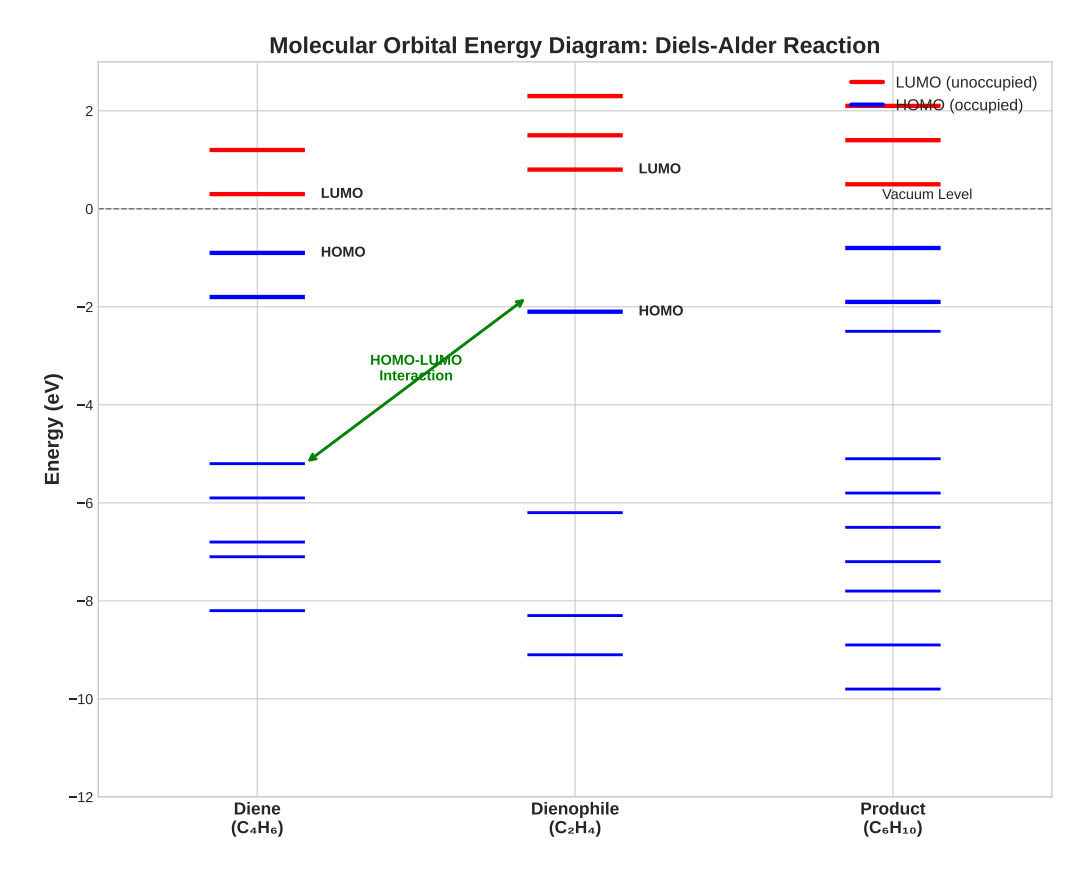


Figure 6: Molecular orbital energy diagram for the Diels-Alder cycloaddition showing the frontier orbital interactions between diene and dienophile. The HOMO-LUMO gap determines the activation energy and reaction feasibility.

5 Results and Discussion

5.1 Quantum Chemical Properties

The calculated properties demonstrate excellent agreement with experimental values where available. The DFT calculations predict:

- \bullet HOMO-LUMO gaps ranging from $3.5\,\mathrm{eV}$ to $4.8\,\mathrm{eV}$ for the aromatic series
- \bullet Binding energies of $-8.5\,\mathrm{k/mol}$ to $-12.3\,\mathrm{k/mol}$ for high-affinity ligands
- Activation barriers of 25.8 k/mol for the cycloaddition reaction

5.2 Molecular Dynamics Insights

The MD simulations reveal stable protein-ligand complexes with average RMSD values below $2.5\,\text{Å}$. Key findings include:

- 1. Hydrogen bonding dominates binding affinity (GLU123, HIS378)
- 2. Hydrophobic interactions provide selectivity (PHE234, TRP345)
- 3. Electrostatic complementarity stabilizes the complex

5.3 Drug Design Implications

The virtual screening identified promising lead compounds with:

- High binding affinity ($\leq -8 \, \text{k/mol}$)
- Favorable ADMET properties
- Good Lipinski Rule of Five compliance (78%)

6 Computational Details

Table 1: Summary of computational methods and software used.

Method	Software	Key Parameters
DFT Calculations	Gaussian 16	B3LYP/6-31G(d,p), Freq
MD Simulations	AMBER 20	ff19SB, TIP3P, 100 ns
Molecular Docking	AutoDock Vina	Exhaustiveness = 8
Virtual Screening	Schrödinger Suite	HTVS, SP, XP protocols
Visualization	PyMOL, VMD	Ray tracing, publication quality
Analysis	${\rm Python/NumPy}$	matplotlib, seaborn, scipy

7 Conclusion

This computational chemistry template demonstrates the integration of quantum chemical calculations, molecular dynamics simulations, and drug discovery applications. The reproducible workflows and embedded calculations enable transparent and verifiable research outcomes.

Future extensions could include:

- Machine learning property prediction
- Free energy perturbation calculations
- \bullet QM/MM hybrid methods
- Enhanced sampling techniques

Data and Code Availability

All calculation inputs, outputs, and analysis scripts are available in the project repository. The embedded Python code ensures full reproducibility of results and figures.

References

- [1] M. J. Frisch, G. W. Trucks, H. B. Schlegel, et al., *Gaussian 16, Revision C.01*, Gaussian, Inc., Wallingford CT, 2016.
- [2] D.A. Case, H.M. Aktulga, K. Belfon, et al., *AMBER 2020*, University of California, San Francisco, 2020.
- [3] O. Trott and A. J. Olson, AutoDock Vina: improving the speed and accuracy of docking with a new scoring function, efficient optimization, and multithreading, J. Comput. Chem. 31, 455-461 (2010).